

Metal-loaded $\text{CeO}_2\text{--ZrO}_2$ solid solutions as innovative catalysts for automotive catalytic converters

Paolo Fornasiero^{a,*}, Gabriele Balducci^a, Jan Kašpar^{*,a}, Sergio Meriani^b,
Roberta di Monte^b, Mauro Graziani^a

^a Dipartimento di Scienze Chimiche, Università di Trieste, Via Giorgieri 1, 34127 Trieste, Italy

^b Dipartimento di Ingegneria dei Materiali e Chimica Applicata, Università di Trieste, Via Valerio 2, 34127 Trieste, Italy

Abstract

The redox behaviour of a $\text{Ce}_{0.5}\text{Zr}_{0.5}\text{O}_2$ solid solution is investigated by means of temperature programmed reduction (TPR) and oxygen uptake measurements. It is shown that the introduction of ZrO_2 into the CeO_2 framework, strongly modifies the reduction behaviour in comparison to pure CeO_2 . Remarkably, in contrast to the CeO_2 , upon repetitive reduction–oxidation processes, the temperature of reduction of the solid solution decreases from 900 to 700 K. The reduction of NO by CO over metal-loaded catalysts is investigated and the role of support Ce^{3+} sites in the enhancing the NO conversion is discussed.

Keywords: $\text{Ce}_{0.5}\text{Zr}_{0.5}\text{O}_2$ redox behaviour of; TPR; NO reduction; Oxygen uptake

1. Introduction

The oxygen storage capacity (OSC) of CeO_2 due to its ability to undergo rapid reduction/oxidation cycles according to the reaction $2\text{CeO}_2 \rightleftharpoons \text{Ce}_2\text{O}_3 + \frac{1}{2}\text{O}_2$; is of relevant technological importance in the automotive exhaust catalysis. Highest simultaneous conversion of the three pollutants CO, hydrocarbons (HC) and NO_x are indeed attained over the three way catalysts (TWCs) only at air/fuel (A/F) ratios close to the stoichiometric values. Excursions to fuel-lean (net oxidizing) and fuel-rich (net reducing) conditions severely decrease respectively NO and CO, HC conver-

sions and high OSC is necessary to minimize these effects [1,2].

Recently, we reported [3] that in the Rh-loaded $\text{CeO}_2\text{--ZrO}_2$ solid solutions the efficiency of the $\text{Ce}^{3+} \rightleftharpoons \text{Ce}^{4+}$ redox cycle is strongly enhanced. Reduction in the bulk of the support occurred at temperatures as low as 600–700 K giving unusually high OSC. Due to the high thermal stability of these materials which were prepared by the ceramic method, i.e., firing a mixture of the oxides at 1873 K, their application to the exhaust catalysis could be of an interest. However, due to the preparation method, the supports were lacking of a high surface area which is usually needed for practical applications. Here, two aspects of these systems are investigated: (i) the redox behaviour of samples of high surface area and the effects

* Corresponding authors. Fax. (+39-40) 6763903.

of thermal ageing and (ii) their effectiveness in the reduction of NO by CO which is key step responsible for the removal of NO from the exhaust.

2. Experimental

The solid $\text{Ce}_{0.5}\text{Zr}_{0.5}\text{O}_2$ solution of high ($64 \text{ m}^2 \text{ g}^{-1}$) surface area was synthesized by a homogeneous gel route according to a previous report [4] by using $\text{Ce}(\text{acac})_4$ and $\text{Zr}(\text{O}-\text{Bu})_4$ as precursors. The dried gel was calcined at 773 K in air for 5 h. CeO_2 (BET surface area $196 \text{ m}^2 \text{ g}^{-1}$) was kindly provided by Dr. Murrel. Supports were impregnated with $\text{RhCl}_3 \cdot 3\text{H}_2\text{O}$ or PdCl_2 precursor to incipient wetness, afterwards the catalysts were dried at 393 K overnight and calcined at 773 K for 5 h. TPR and O_2 uptake measurements were carried out as previously described [3]. To minimize contribution from adsorbed species, prior to the TPR, the samples were treated in He at 900 K for 5 h. A typical reduction–oxidation cycle was carried out as follows: TPR (H_2 (5%) in Ar, 25 ml min^{-1} , 10 K min^{-1}) up to 1273 K and then degassed at 1273 K in He for 30 min, O_2 uptake was measured at 700–500 K. Catalytic experiments were carried out in a U-shaped quartz flow-reactor (NO (1%) and CO (3%) in He, total flow 30 ml min^{-1} , GHSV = $12500\text{--}50000 \text{ h}^{-1}$).

3. Results and discussion

Fig. 1 reports the TPR profiles of fresh $\text{Ce}_{0.5}\text{Zr}_{0.5}\text{O}_2$ (BET area $64 \text{ m}^2 \text{ g}^{-1}$) and the effects of subsequent reduction–oxidation cycles. For comparison, the same experiment carried out on CeO_2 (BET area $196 \text{ m}^2 \text{ g}^{-1}$) is also included.

For reader's convenience TPR of CeO_2 is discussed first: fresh CeO_2 features two peaks at 790 and 1100 K (Fig. 1, trace 4) associated with surface and bulk reduction [2,5], respec-

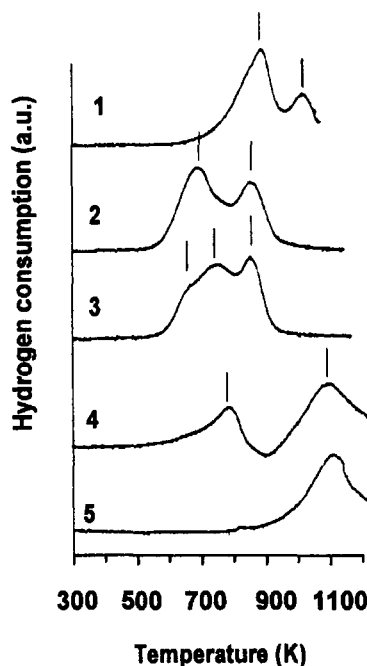


Fig. 1. TPR profile of (1) fresh $\text{Ce}_{0.5}\text{Zr}_{0.5}\text{O}_2$ and (2–3) recycled 1 and 7 times, respectively; (4) fresh CeO_2 and (5) recycled 2 times.

tively, even if reversible H_2 fixation [6] and/or formation of H_2 bronzes [7] cannot be excluded for the former peak. After ageing at 1273 K and oxidation at 700 K, in the subsequent TPR almost no reduction below 900 K is observed (Fig. 1, trace 5). Repetitive oxidation–reduction cycles do not modified further this behaviour. The absence of the peak at 790 K is consistent with a collapse of surface area upon reduction (see below). Above 673 K, CeO_2 surface is not stable in the presence of H_2 [8].

The comparison with TPR profiles of $\text{Ce}_{0.5}\text{Zr}_{0.5}\text{O}_2$ is significant. The TPR of fresh $\text{Ce}_{0.5}\text{Zr}_{0.5}\text{O}_2$ shows two peaks at 880 and 1010 K (Fig. 1, trace 1). After ageing at 1273 K and oxidation at 700 K, in the subsequent experiment, the TPR profile is modified, the peaks at 880 and 1010 K disappear and new broad features are observed at lower temperatures (690 and 850 K) (Fig. 1, trace 2). Upon further recycling of the sample through repetitive reduction–oxidation cycles, the TPR profile still modifies to reach a final appearance with peaks at 850, 740 and a shoulder at 660 K (Fig. 1,

trace 3). The whole reduction is complete by 950 K. The H_2 consumption estimated from the TPR and the O_2 uptake are roughly equivalent suggesting that contribution from adsorbed species are relatively unimportant in the present samples. The attribution of the reduction peaks at 880 and 1010 K in the fresh sample is not straightforward: a H_2 consumption of $7.6 \cdot 10^{-4} \mu\text{mol g}^{-1}$ is measured for the former peak which is about 2.5 times that estimated for surface reduction according to [5] suggesting that, at variance with CeO_2 , there is no net distinction between the surface and bulk reduction. Consistently, we showed [3] that incorporation of ZrO_2 into the CeO_2 framework strongly promoted the oxygen mobility in the bulk of the solid solution. A perusal of the effects of recycling of $\text{Ce}_{0.5}\text{Zr}_{0.5}\text{O}_2$ through reduction–oxidation cycles reveals that the strongest modification of the TPR profiles occurred after the first cycle. In the subsequent cycles, the temperatures of the maximum of the peaks/shoulder at 850, 690 and 660 K appear to be scarcely affected. The modification of the TPR profiles could be ascribed primarily to a modification of the relative intensity of the peak/shoulder at 690 and 660 K. Presence of two peaks at 600–950 and 1050–1250 K due to the reduction of the support in the bulk were previously observed in the TPR of $\text{Rh/Ce}_x\text{Zr}_{1-x}\text{O}_2$ ($x = 0.5\text{--}0.9$) of a low surface area (about $1 \text{ m}^2 \text{ g}^{-1}$) [3]. Observation of three features in the TPR profile suggests that the shoulder at 660 K should be ascribed to surface reduction. Consistently, by fitting the TPR profile reported in trace 3 of Fig. 1 with three Gaussian functions [5], a consumption of $4.5 \times 10^{-5} \mu\text{mol g}^{-1}$ can be estimated for the shoulder at 660 K which compares well with the value $5.3 \times 10^{-5} \mu\text{mol g}^{-1}$ calculated according to [5] for a surface area of $12 \text{ m}^2 \text{ g}^{-1}$ (see below). Apparently, in the sintered samples the surface reduction is favoured over the bulk. Noteworthy is that the surface reduction shifts to lower temperature in the sintered samples compared to the fresh one.

Bulk diffusion is rate limiting the reduction

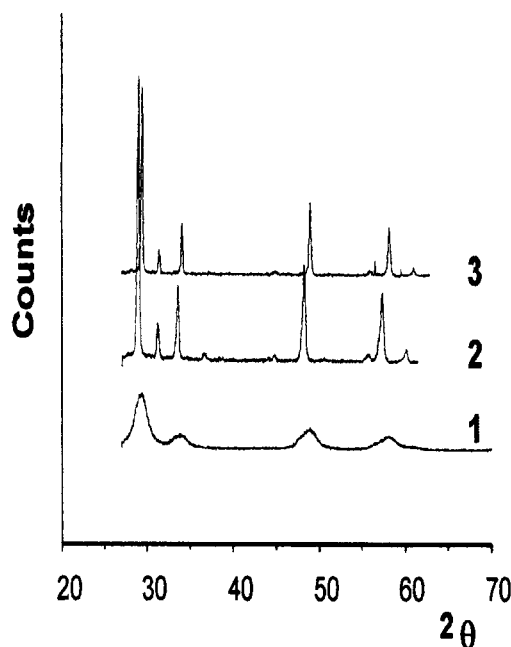


Fig. 2. XRD patterns of (1) fresh, (2) reduced and (3) oxidized $\text{Ce}_{0.5}\text{Zr}_{0.5}\text{O}_2$.

process in the bulk [3]. On increasing the degree of reduction during the TPR, the concentration of the positively and negatively charged defects created by the reduction progressively increases. At a certain point, their concentration will be high enough to favour the clustering. This will make the ionic transport more difficult, slowing down the reduction process. Further reduction will occur only at higher temperatures, thus, accounting for the observation of two peaks due to the reduction in the bulk.

As shown in Fig. 2, XRD pattern of the fresh $\text{Ce}_{0.5}\text{Zr}_{0.5}\text{O}_2$ features broad peaks which are successfully indexed in the cubic $\text{Fm}\bar{3}\text{m}$ group. A cell parameter of 5.26 \AA is obtained. For comparison, CeO_2 shows a cell parameter of 5.41 \AA . After reduction, all the peaks are significantly narrowed revealing an extensive sintering of the sample and the cell parameter increases to 5.34 \AA due to the higher ionic diameter of Ce^{3+} (1.10 \AA) compared to Ce^{4+} (0.97 \AA). After oxidation at 700 K, cubic structure is retained and the cell parameter decreases back to 5.26 \AA . This behaviour is observed in all the

subsequent treatments. Similarly, the XRD patterns of the CeO_2 subjected to a reduction–oxidation cycle revealed an extensive sintering of the sample. An expansion of the lattice parameter of 2.8% was observed after a reduction at 1073 K [5]. Modification of the texture upon thermal and redox treatments was investigated by nitrogen adsorption at 77 K. Upon thermal treatment under N_2 or calcination in air up to 900 K, BET surface area decreased from 196 to 155 and from 64 to 42 $\text{m}^2 \text{g}^{-1}$ for CeO_2 and $\text{Ce}_{0.5}\text{Zr}_{0.5}\text{O}_2$, respectively. In contrast, a treatment in H_2 at 900 K declines the BET areas to respectively 30 and 13 $\text{m}^2 \text{g}^{-1}$ which suggests that the reducing treatment strongly favours the sintering of both $\text{Ce}_{0.5}\text{Zr}_{0.5}\text{O}_2$ and CeO_2 compared to a simple thermal treatment. Notably, also the texture of both $\text{Ce}_{0.5}\text{Zr}_{0.5}\text{O}_2$ and CeO_2 is affected by the redox treatments: after reduction at 1000 K and subsequent oxidation at 700 K, the BET surface areas decrease to 12 $\text{m}^2 \text{g}^{-1}$ and the average pore diameters calculated according to Ref. [9] from the desorption isotherm, increase for the two samples respectively from 3.4 to 14.9 and from 4.0 to 11.9 nm. Sintering of the samples with concurrent formation of mesoporosity is clearly confirmed by SEM. We suggests that contraction–expansion of the cell

parameter is responsible for the latter phenomenon. The parallel evolution of the texture of both $\text{Ce}_{0.5}\text{Zr}_{0.5}\text{O}_2$ and CeO_2 also suggests that it should not be responsible for the promotion of the reducibility of the former sample upon sintering. An alternative explanation is therefore needed.

The role of ZrO_2 in promoting the bulk oxygen diffusion is established [3]. As far as the surface processes are concerned, it should be observed that H_2 dissociation with formation of supplementary OH groups was observed over CeO_2 surface above 473 K [5]. Dissociation of H_2 occurred over degassed ZrO_2 surfaces already at rt [10]. The higher ionic character of the Zr–O bond compared to the Ce–O favours the polarization of the homo and lumo orbitals of adsorbed H_2 making its dissociation easier [11]. Upon thermal treatment, ZrO_2 surface shows a depletion of oxygen at the surface generating Lewis type acidity [12] which could further favour H_2 activation. Accordingly, we infer that on increasing the temperature during the TPR experiment, progressive elimination of surface OH groups will occur which generates surface sites of strong Lewis acidity. These sites may play a role in H_2 activation accounting for lower temperature for surface reduction upon

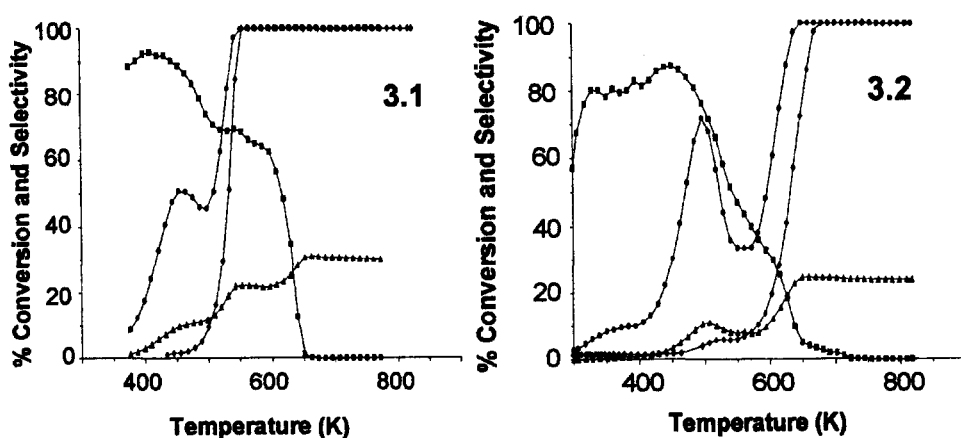


Fig. 3. NO–CO reaction over freshly reduced (3.1) Rh- and (3.2) Pd-loaded $\text{Ce}_{0.5}\text{Zr}_{0.5}\text{O}_2$: (●) NO conversion, (▲) CO conversion and (■) selectivity in N_2O formation; (3.1) (◆) NO conversion over Rh/ $\text{Ce}_{0.5}\text{Zr}_{0.5}\text{O}_2$ partially deactivated at 900 K in NO + CO; (3.2) (◆) NO conversion over Pd/ $\text{Ce}_{0.5}\text{Zr}_{0.5}\text{O}_2$ partially deactivated at 900 K in NO + CO. Reaction conditions as reported in the Experimental section.

recycling of the $\text{CeO}_2\text{--ZrO}_2$ catalyst. On the other hand, during the TPR of the fresh sample collapse of surface area and pore filling occur concurrently with the reduction which could further slow the reduction process.

Summarizing, the $\text{Ce}_{0.5}\text{Zr}_{0.5}\text{O}_2$ solid solution appears as an interesting material for the TWCs due to its ability to sustain an efficient $\text{Ce}^{3+} \leftrightarrow \text{Ce}^{4+}$ redox cycle even after extensive sintering. This is an important point in view of previous observation that NO is efficiently decomposed over reduced ceria containing catalysts [3]. We have therefore investigate the effectiveness of the Rh and Pd-loaded $\text{CeO}_2\text{--ZrO}_2$ samples for the reduction of NO by CO which, as above stated, is a key reaction responsible for the removal of NO from the automotive exhaust. The results obtained are summarized here, a detailed discussion is reported elsewhere. TPR and XANES measurements at the Ce L_{III} edge showed that in the Rh- and Pd-loaded $\text{Ce}_{0.5}\text{Zr}_{0.5}\text{O}_2$, the support reduction occurs concurrently with the reduction of the noble metal oxide. The effects of reduction on the activity in the CO–NO reduction are illustrated in Fig. 3.

In the freshly reduced samples and below 500 K, the reactant conversions are significantly enhanced in comparison to the catalysts which have been used in the NO–CO above 500 K (see Fig. 3). Conversely, a Rh/ Al_2O_3 catalyst showed an activity comparable to the latter case. Notably, in the freshly reduced catalysts, the light-off temperatures (50% conversion) are lowered by 50–100 K. Independent temperature programmed NO decomposition measurements carried out on Rh-loaded and metal-free $\text{Ce}_{0.5}\text{Zr}_{0.5}\text{O}_2$ of low and high surface area showed that NO is dissociated at surface Ce^{3+} sites already at 298 K. In contrast, in the low surface area samples, reoxidation by NO of the bulk of the support occurs at about 500 K. This suggests that surface oxygen vacancies generated by the reduction are immediately annihilated by the reaction with NO and should not be responsible for the enhanced activity of the freshly reduced catalysts. As recently suggested

by Serre et al. [13], an oxygen vacancy gradient which is generated by the bulk oxygen vacancies, may provide the driving force for the dissociation of the NO at the support, resulting in enhanced catalytic activity. On increasing the temperature above 500 K, the oxygen mobility in the bulk will also increase which will fully reoxidize the support. The role of the support in the conversion of NO is substantiated by the product distribution in the NO–CO reaction at 473 K: selectivity in N_2O formation of 86% and 87% is observed for Rh- and Pd- loaded $\text{Ce}_{0.5}\text{Zr}_{0.5}\text{O}_2$ respectively. These observations suggest a new role for the metal component, i.e., that of favouring the regeneration of Ce^{3+} sites in the reaction conditions. These sites, in turn, efficiently decompose NO, resulting in enhanced catalytic activities.

Acknowledgements

Authors thank Dr. G. Gubitosa, Gilardini Silenziamento S.p.A., for helpful discussions. The Ministero dell'Università e della Ricerca Scientifica (MURST-Roma) and University of Trieste are acknowledged for financial support.

References

- [1] J.C. Summers and S.A. Ausen, *J. Catal.*, 58 (1979) 131; G. Kim, *Ind. Eng. Chem. Prod. Res. Dev.*, 21 (1982) 267; K.C. Taylor, *Catal. Sci. Technol.*, 5 (1984).
- [2] H.C. Yao and Y.-F. Yu Yao, *J.Catal.*, 86 (1984) 254.
- [3] G. Ranga Rao, J. Kašpar, S. Meriani, R. Di Monte and M. Graziani, *Catal. Lett.*, 24 (1994) 107; P. Fornasiero, R. Di Monte, G. Ranga Rao, J. Kašpar, S. Meriani, A. Trovarelli and M. Graziani, *J.Catal.*, 151 (1995) 168; G. Ranga Rao, P. Fornasiero, J. Kašpar, S. Meriani, R. Di Monte and M. Graziani, *Stud. Surf. Sci. Catal.*, 96 (1995) 631.
- [4] S. Meriani and G. Soraru, in P. Vicenzini (Editor), *Ceramic Powders*, Elsevier, Amsterdam, 1983, pp. 547–554.
- [5] A. Laachir, V. Perrichon, A. Badri, J. Lamotte, E. Catherine, J.C. Lavalley, J. El Fallah, L. Hilaire, F. le Normand, E. Quemere, N.S. Sauvion and O. Touret, *J. Chem. Soc., Faraday Trans.*, 87 (1991) 1601; V. Perrichon, A. Laachir, G. Bergeret, R. Frety and L. Tournayan, *J. Chem. Soc., Faraday Trans.*, 90 (1994) 773.

- [6] J.L.G. Fierro, J. Soria, J. Sanz and J.M. Rojo, *J. Solid State Chem.*, 66 (1987) 154.
- [7] S. Bernal, J.J. Calvino, G.A. Cifredo, J.M. Gatica, J.A. Perez Omil and J.M. Pintado, *J. Chem. Soc., Faraday Trans.*, 89 (1993) 3499.
- [8] J. El Fallah, S. Boujana, H. Dexpert, A. Kiennemann, J. Majerus, O. Touret, F. Villain and F. Le Normand, *J. Phys. Chem.*, 98 (1994) 5522.
- [9] E.P. Barret, L.G. Joyner and P.P. Halenda, *J. Am. Chem. Soc.*, 73 (1951) 373.
- [10] J. Kundo, H. Abe, Y. Sakata, K. Maruya, K. Domen and T. Onishi, *J. Chem. Soc., Faraday Trans.*, 84 (1988) 511.
- [11] H. Nakatsuji, M. Hada, H. Ogawa, K. Nagata and K. Domen, *J. Phys. Chem.*, 98 (1994) 11840.
- [12] H.J.M. Bosman, E.C. Kruissink, J. van der Spoel and F. van den Brink, *J. Catal.*, 148 (1994) 660.
- [13] C. Serre, F. Garin, G. Belot and G. Maire, *J. Catal.*, 141 (1993) 9.